NRC Research Press

ARTICLE

Mechanism of atrazine resistance in atrazine- and HPPD inhibitor-resistant Palmer amaranth (*Amaranthus palmeri* S. Wats.) from Nebraska

Parminder S. Chahal, Mithila Jugulam, and Amit J. Jhala

Abstract: Palmer amaranth (*Amaranthus palmeri* S. Wats.) is one of the most problematic weed species in agronomic crops in the United States. A Palmer amaranth biotype multiple-resistant to atrazine and 4-hydroxyphenylpyruvate dioxygenase (HPPD) inhibitors was reported in a seed corn production field in Nebraska. Rapid detoxification mediated by cytochrome P450 monooxygenases and increased HPPD gene expression were reported as the mechanisms of mesotrione resistance in atrazine- and HPPD inhibitor-resistant Palmer amaranth biotype from Nebraska; however, the mechanism of atrazine resistance is unknown. The objectives of this study were to investigate target site or non-target site based mechanisms conferring atrazine resistance in Palmer amaranth from Nebraska. ^{14}C-atrazine absorption and translocation studies revealed that reduced atrazine absorption or translocation were not involved as one of the mechanisms of atrazine resistance. Instead, greater ^{14}C-atrazine absorption and recovery in treated leaves were observed in resistant compared with susceptible Palmer amaranth. No known mutations including $Ser_{264}Gly$ substitution in the *psbA* gene causing target site based atrazine resistance were observed. However, the parent ^{14}C-atrazine was metabolized rapidly <4 h after treatment in resistant plants, conferring enhanced atrazine metabolism as the mechanism of resistance.

Key words: atrazine, herbicide absorption/translocation, herbicide metabolism, Palmer amaranth, target site, non-target site.

Résumé : L'amarante de Palmer (*Amaranthus palmeri* S. Wats.) est l'adventice qui pose le plus de problèmes aux agriculteurs des États-Unis. Un biotype de cette mauvaise herbe, résistant à l'atrazine et aux inhibiteurs de la 4-hydroxyphénylpyruvate dioxygénase (HPPD), a été signalé dans un champ de maïs-semences du Nebraska (É.-U.). La résistance de ce biotype à la mésotrione semble dériver d'une détoxification rapide entraînée par les mono-oxygénases du cytochrome P450 et par une meilleure expression du gène HPPD. Cependant, on ignore d'où vient la résistance à l'atrazine. Les chercheurs souhaitaient approfondir les mécanismes susceptibles d'agir aux sites visés ou pas et d'avoir rendu l'amarante de Palmer du Nebraska résistante à l'atrazine. Les études sur l'absorption et la translocation de l'atrazine marquée au ^{14}C révèlent que la résistance à cet herbicide ne résulte pas moins forte absorption ou translocation. Au contraire, les auteurs ont observé une absorption plus importante de l'atrazine marquée au ^{14}C et ont plus récupéré d'herbicide dans les feuilles traitées des plants résistants que dans celles des plants sensibles. Les chercheurs n'ont pas non plus relevé de mutations connues, par exemple la substitution de $Ser_{264}Gly$ dans le gène *psbA* expliquant la résistance à l'atrazine aux sites visés. Toutefois, les plants résistants ont métabolisé rapidement la ^{14}C-atrazine mère, soit en moins de quatre heures, ce qui laisse supposer que le mécanisme à l'origine de la résistance est un métabolisme plus efficace de l'herbicide. [Traduit par la Rédaction]

Mots-clés : atrazine, absorption/translocation d'herbicide, métabolisme des herbicides, amarante de Palmer, site visé, site non visé.

Received 22 October 2018. Accepted 26 March 2019.

P.S. Chahal and A.J. Jhala.* Department of Agronomy and Horticulture, University of Nebraska-Lincoln, Lincoln, NE 68583, USA.

M. Jugulam. Department of Agronomy, Kansas State University, Manhattan, KS 66506, USA.

Corresponding author: Amit J. Jhala (email: Amit.Jhala@unl.edu).

*A.J. Jhala currently serves as an Associate Editor; peer review and editorial decisions regarding this manuscript were handled by Robert Gulden.

Introduction

Palmer amaranth (*Amaranthus palmeri* S. Wats.) is a C_4 dioecious species and is one of the most troublesome weeds in US agriculture (Chahal et al. 2015; Kohrt and Sprague 2017). Palmer amaranth has evolved resistance to different herbicide sites of action in the United States, including microtubule, acetolactate synthase (ALS), photosystem (PS) II, 5-enol-pyruvylshikimate-3-phosphate synthase (EPSPS), hydroxyphenylpyruvate dioxygenase (HPPD), and protoporphyrinogen oxidase (PPO) inhibitors (Heap 2018). A Palmer amaranth biotype resistant to PS II inhibitors (atrazine) as well as HPPD inhibitors such as isoxaflutole, mesotrione, tembotrione, and topramezone applied preemergence (PRE) or postemergence (POST) was confirmed in a seed corn production field in Nebraska (Jhala et al. 2014; Chahal and Jhala 2018). Nakka et al. (2017*b*) reported rapid detoxification mediated by cytochrome P450 monooxygenases and increased expression of the HPPD gene as the mechanisms conferring mesotrione resistance in the atrazine- and HPPD inhibitor-resistant Palmer amaranth biotype from Nebraska. Similarly, Küpper et al. (2018) reported rapid tembotrione metabolism or detoxification causing tembotrione resistance in the same Nebraska Palmer amaranth biotype; however, information about the mechanism conferring atrazine resistance in this biotype is missing.

Plastoquinone acts as an electron acceptor during the light reaction phase of photosynthesis, and PS II inhibitors such as atrazine compete with plastoquinone and binds itself at the Q_B binding site of the D1 protein, which results in the inhibition of electron transport chain (Hess 2000). Electron transport chain inhibition causes the accumulation of reactive oxygen species, singlet chlorophyll, and triplet chlorophyll species, causing damage to the D1 protein (Hess 2000). Since the *psbA* gene encodes the D1 protein in PS II, any mutation in this gene affects the binding ability of atrazine at the Q_B site of the D1 protein, and ultimately results in atrazine resistance in the plant. Previous studies have reported point mutations in the *psbA* gene as the most common mechanism of atrazine resistance in different weed species such as barnyardgrass [*Echinochloa crus-galli* (L.) P. Beauv.] (Lopez-Martinez et al. 1997), large crabgrass [*Digitaria sanguinalis* (L.) Scop.] (Salava et al. 2008), and wild radish (*Raphanus raphanistrum* L.) (Shane Friesen and Powles 2007). The most commonly reported point mutation in the *psbA* gene is $Ser_{264}Gly$ (Shane Friesen and Powles 2007). In addition, enhanced atrazine detoxification or metabolism due to tripeptide glutathione (GSH) conjugation has also been reported as the mechanism conferring non target site atrazine resistance in common waterhemp and Palmer amaranth (Gray et al. 1996; Ma et al. 2013; Huffman et al. 2015; Nakka et al. 2017*a*). GSH conjugation with atrazine catalyzed by glutathione *S*-transferase (GST) results in the formation of GS-atrazine, which is relatively nonphytotoxic, making plants resistant to atrazine application (Gray et al. 1996; Ma et al. 2013). Svyantek et al. (2016) reported reduced atrazine absorption and translocation along with enhanced atrazine metabolism as the mechanisms of resistance in annual bluegrass (*Poa annua* L.).

The objectives of this study were to (*i*) determine the absorption, translocation, or metabolism of ^{14}C atrazine, and (*ii*) sequence the *psbA* gene in atrazine- and HPPD inhibitor-resistant and -susceptible Palmer amaranth from Nebraska to identify any target site or non-target site based atrazine resistance.

Materials and Methods

^{14}C-atrazine absorption and translocation studies

Seeds of resistant Palmer amaranth were collected from a grower's field already confirmed with the presence of atrazine- and HPPD inhibitor-resistant Palmer amaranth in Fillmore County, NE (Jhala et al. 2014). Seeds of susceptible Palmer amaranth were collected from a grower's field in Buffalo County, NE, with no history of atrazine or HPPD inhibitors applications. Palmer amaranth seeds were planted in separate germination trays containing the potting mix under greenhouse conditions at Kansas State University, Manhattan, KS. Plants achieving 2–4 cm height were later transplanted into square plastic pots (8 cm × 8 cm × 10 cm) containing potting mix under same greenhouse conditions. A day/night temperature regime of 30 °C/22 °C was maintained in the greenhouse with a 16 h photoperiod and sodium vapor lamps with an illumination density of 250 μmol m^{-2} s^{-1} were used to provide supplemental light. In this study, plants were treated with radiolabeled atrazine herbicide and there were entry restrictions for radiolabeled treated plants in the greenhouse. Therefore, at 7 d after transplanting, plants were transferred to a growth chamber maintained at 30 °C/20 °C day/night temperatures with a 16 h photoperiod and 75% relative humidity after herbicide applications.

One millilitre of ^{14}C-atrazine working solution was prepared by mixing 90 μL of ^{14}C-atrazine water solution (3.3 kBq with a specific activity of 160 mCi $mmol^{-1}$), 25 μL of Aatrex herbicide, 25 μL AMS, 10 μL COC, and 850 μL of water, which is equivalent to 2240 g a.i. of atrazine in 187 L ha^{-1} volume. Six Palmer amaranth plants reaching a height of 10–12 cm were treated with 10 μL ^{14}C-atrazine solution per plant with a total of ten 1-μL droplets on the upper surface of the fully expanded fourth youngest leaf using a Wiretrol® (10 μL, Drummond Scientific Co., Broomall, PA). The treated plants were later moved to the same growth chamber within 20 min after treatment. At 4, 8, 24, 48, and 72 h after treatment (HAT), plants (six plants for each HAT) were dissected into leaves above the treated leaf (ATL), the treated leaf (TL), leaves and stems below the treated leaf (BTL), and roots. The treated plants in the

experiment were laid out using a randomized complete block design with six replications. The experiment was subsequently repeated using the same procedure.

To remove the unabsorbed herbicide from the TL surface, the TL was rinsed twice for 1 min in a scintillation vial containing 5 mL of wash solution (10% *v*/*v* ethanol aqueous solution with 0.5% of Tween-20). The rinse in the scintillation vial was then mixed with 15 mL of scintillation cocktail [Ecolite-(R), MP Biomedicals, LLC., Santa Ana, CA]. The radioactivity in the final leaf rinse solution was determined by using liquid scintillation spectrometry (LSS) (Beckman Coulter LS6500 Multipurpose Scintillation Counter, Beckman Coulter Inc., Brea, CA). All plants parts (TL, ATL, BTL, and roots) were wrapped separately in a single layer of tissue paper and then dried in an oven maintained at 60 °C for 48 h. The dried plant parts were later combusted for 3 min using a biological oxidizer (OX-501, RJ Harvey Instrument Corp., Tappan, NY) to recover the radiolabeled herbicide in a ^{14}C-trapping scintillation cocktail, and later radioactivity was determined using LSS. The equations used in the literature to calculate percent herbicide absorption and translocation (Godar et al. 2015; Ganie et al. 2017*a*) were modified and used for this study:

$$(1)\quad \%\ \text{Absorption} = \left[\left(\frac{\text{Total radioactivity applied} - \text{Radioactivity recovered in wash solution}}{\text{Total radioactivity applied}}\right) \times 100\right]$$

$$(2)\quad \%\ \text{Radioactivity in the treated leaf} = \frac{\text{Radioactivity recovered in the treated leaf}}{\text{Total radioactivity applied}} \times 100$$

$$(3)\quad \%\ \text{Radioactivity above the treated leaf} = \frac{\text{Radioactivity recovered above the treated leaf}}{\text{Total radioactivity applied}} \times 100$$

$$(4)\quad \%\ \text{Radioactivity below the treated leaf} = \frac{\text{Radioactivity recovered below the treated leaf}}{\text{Total radioactivity applied}} \times 100$$

$$(5)\quad \%\ \text{Translocation} = \frac{\text{Total radioactivity recovered above + below the treated leaves + roots}}{\text{Total radioactivity applied}} \times 100$$

^{14}C-atrazine metabolism study

Resistant and susceptible Palmer amaranth biotypes were grown under greenhouse conditions and later moved to a growth chamber as described in ^{14}C-atrazine absorption and translocation studies. Six Palmer amaranth plants reaching 10–12 cm in height were treated with a total of 20 μL of 6.7 kBq ^{14}C-atrazine solution (10 μL each on the fourth and fifth youngest leaves), which is equivalent to 2240 g atrazine ha^{-1}. Treated plants were later moved to a growth chamber. At 4, 8, 24, and 48 HAT, the TL was dissected from each treated plant (six treated plants for each HAT) and rinsed for 1 min in a scintillation vial containing 5 mL of wash solution to remove the unabsorbed radiolabeled herbicide from the TL surface. The rinsed TL was ground in liquid nitrogen (−195.79 °C) using a pre-chilled mortar and pestle.

The extraction of the parent ^{14}C-atrazine and its major metabolites was initiated by incubating ground TL tissue in 15 mL of 90% acetone in a freezer at 4 °C for 16 h and later centrifuging at 6500 rev min^{-1} for 10 min. The collected supernatant was concentrated to a final volume of 100–600 μL by evaporating in a rotary evaporator (Centrivap, Labconco, Kansas City, MO) maintained at 50 °C for 2–2.5 h. The concentrated supernatant was transferred to a 1500 μL centrifuge tube and centrifuged at 13 000 rev min^{-1} for 10 min. The radioactivity of each sample in a 1500 μL centrifuge tube was measured using LSS. The samples were later normalized to 3000 dpm 50 μL^{-1} (60 dpm = 1 Bq) using 50% acetonitrile (ThermoFisher Scientific, Waltham, MA). The normalized samples in 50 μL tubes were fed into a reverse phase high performance liquid chromatography (HPLC) system (System Gold, Beckman Coulter, Pasadena, CA) to separate the parent ^{14}C-atrazine and the conjugated metabolites. A synthetic atrazine-GSH conjugate was also synthesized by incubating 20 mmol L^{-1} of GSH at 35 °C for 24 h with 0.1 mmol L^{-1} of ^{14}C-atrazine in 60 mmol L^{-1} of 3-[2-hydroxy-1,1-bis(hydroxymethyl)ethyl] amino-1-propanesulfonic acid (TAPS) buffer with a pH of 9.5. As well, 0.1 mmol L^{-1} of ^{14}C-atrazine without the addition of GSH was also incubated in 60 mmol L^{-1} TAPS buffer at similar conditions as described above for the atrazine-GSH conjugate. A reverse-phase HPLC was used to determine the retention times of the GSH-^{14}C-atrazine conjugate, parent ^{14}C-atrazine compound, and parent ^{14}C-atrazine recovered in resistant as well as susceptible Palmer amaranth samples. Reverse-phase HPLC was done using a Zorbax SAX column of 4.6 mm × 250 mm and 5 μm particle size (Agilent Technologies, Santa Clara, CA) at a 1 mL min^{-1} flow rate with eluent A (water mixed with 0.1% trifluoroacetic acid) and eluent B (acetonitrile mixed with 0.1% trifluoroacetic acid) at a pressure of ~350 bars (Godar et al. 2015; Nakka et al. 2017*a*). Radiolabeled compounds in the samples were detected using a radioflow detector (EG&G Berthold, LB 509, Berthold Technologies, Bad Wildbad, Germany) and Ultima-Flo M cocktail (PerkinElmer, Inc., Waltham, MA).

Table 1. Comparison of AICc values for the nonlinear and linear regression models to fit the best model for predicting ^{14}C-atrazine absorption and translocation and ^{14}C-atrazine metabolism in studies conducted at Kansas State University, Manhattan, KS.

	^{14}C-atrazine absorption and translocation study		^{14}C-atrazine metabolism study	
Regression models[a]	^{14}C-atrazine absorption	^{14}C-atrazine present in treated leaf	Parent ^{14}C-atrazine present in treated leaf	^{14}C-metabolite present in treated leaf
Two-parameter rectangular hyperbolic function	803	1532	411	348
Two parameter asymptotic function	831	1548	413	349
Three-parameter log-logistic function	885	1623	407	285
Linear function	1112	2086	397	297

Note: AICc, corrected information-theoretic model comparison criterion.
[a]Regression models with the lowest AICc values were selected to best describe the ^{14}C-atrazine absorption and translocation or ^{14}C-atrazine metabolism data.

The experiment was repeated after completion of the first run using the same procedure under similar growing conditions.

Sequence of *psbA* gene

Young leaf tissue of 10 resistant Palmer amaranth plants which survived the label rate (2240 g ha^{-1}) and twice (4480 g ha^{-1}) the label rate of atrazine was harvested along with nontreated susceptible Palmer amaranth plants. The harvested sample was flash frozen using liquid nitrogen and then ground into a fine powder in liquid nitrogen. The genomic DNA from the powdered samples was extracted using a DNeasy Plant Mini Kit (Qiagen, Hilden, Germany) following the manufacturer's protocol. Before performing the polymerase chain reactions (PCRs), the quality and quantity of the DNA was analyzed using 0.8% agarose gel electrophoresis and nanodrop (NanoDrop 1000, ThermoFisher Scientific), respectively. PCRs were performed on the genomic DNA using a T100™ Thermal Cycler (Bio-Rad Inc., Hercules, CA) to amplify the mutations known in the *psbA* gene by using 80 ng of genomic DNA with the primers used by Mengistu et al. (2005) and a PCR master mix (Promega, Madison, WI). The conditions for PCR included initial denaturation at 94 °C for 4 min followed by 40 cycles of denaturation at 94 °C for 30 s, primer annealing at 55 °C for 30 s, product extension at 72 °C for 45 s, and a final extension cycle at 72 °C for a total of 7 min. The PCR products were sequenced by GENEWIZ (GENEWIZ Inc., South Plainfield, NJ) and DNA sequences from the resistant and susceptible biotypes were aligned and analyzed using MultAlin software to detect the presence of mutation in the target site.

Statistical analysis

^{14}C-atrazine absorption or translocation, and data for the parent ^{14}C-atrazine or its metabolites, were subjected to analysis of variance (ANOVA) using PROC GLIMMIX in SAS version 9.3 (SAS Institute Inc., Cary, NC). Data were analyzed using a normal distribution using the identity-link function. Experimental runs, biotype, and HAT were considered the fixed effects and replication was a random effect in the model. Data were combined over experimental runs when there was no effect of experimental run or interaction with biotype or HAT. Where the ANOVA indicated that biotype and HAT effects or their interactions were significant, means were separated at $P \leq 0.05$ with the Tukey–Kramer's pairwise comparison test.

Regression analysis was performed for the ^{14}C-atrazine absorption or translocation and the parent ^{14}C-atrazine and its metabolites present in TL over time using R software (R statistical software, R Foundation for Statistical Computing, Vienna, Austria). Nonlinear regression models such as a two-parameter rectangular hyperbolic function, a two parameter asymptotic regression function, or a three-parameter log-logistic function were fitted to data using the drm function in the drc package (drc 2.3, Ritz and Strebig 2016; R 3.1.1, Kurt Hornik) in R software (R version 3.3.1, R Foundation for Statistical Computing), and a linear regression model was fitted using the lm function in the STATS package in R software (Kniss et al. 2011). The above-fitted models were compared using the corrected information-theoretic model comparison criterion (AICc) in R software, and the models with the lowest AICc values were selected to best describe the data (Table 1). Using the AIC approach, a two-parameter rectangular hyperbolic function was fitted to ^{14}C-atrazine absorption or ^{14}C-atrazine present in the TL:

$$(6) \qquad \mathrm{RH} = (R_{\max} \times t)/[(10/c) \times t_c + t]$$

where RH describes the ^{14}C-atrazine absorption or ^{14}C-atrazine present in the TL, $R_{\max}$ is the maximum

percentage of applied herbicide dose that was absorbed, translocated, or present in the TL at the time (t), c represents an arbitrary percentage (90% in this study) of A_{max}, and t_c represents the number of HAT required to reach 90% of the R_{max}.

A three parameter log-logistic model was fitted to the parent ^{14}C-atrazine remaining in the TL in the metabolism study:

$$(7) \qquad Y = \frac{A_{max}}{1 + \exp[b(\log t - \log £)]}$$

where Y is the parent ^{14}C-atrazine remaining in the TL (% of recovered), A_{max} is the maximum percentage of the parent ^{14}C-atrazine present in the TL (% of recovered) at time (t), £ represents the number of HAT required to reach 90% of the A_{max}, and b represents the relative slope around the parameter £.

A linear model was fitted to the ^{14}C-atrazine metabolites recovered in the TL in the metabolism study:

$$(8) \qquad Y = \alpha x + \beta$$

where Y is the percentage of ^{14}C-atrazine metabolites recovered in the TL, α is the slope or rate of change of the ^{14}C-atrazine metabolite recovery over hours, x is the time expressed as HAT, and β is the intercept or initial ^{14}C-atrazine metabolite expressed as the percentage recovered. The predicted parameters in the fitted regression models were compared among resistant and susceptible biotypes using a t test in R software.

Results and Discussion

^{14}C-atrazine absorption and translocation

No effect of experimental runs or its interaction with biotype or HAT was observed for ^{14}C-atrazine absorption and translocation, and for ^{14}C-atrazine recovered in ATL, TL, and BTL; therefore, data were combined over two experimental runs (data not shown). There was a significant biotype-by-HAT interaction for ^{14}C-atrazine absorption and ^{14}C-atrazine recovered in the TL; therefore, regression analysis was performed for both biotypes over HAT. No effect of biotype, HAT, or their interaction was observed on ^{14}C-atrazine translocation or ^{14}C-atrazine recovery in the ATL and BTL (data not shown); therefore, regression analysis was not performed.

A two-parameter rectangular hyperbolic model predicted overall greater (89% of applied) absorption of ^{14}C-atrazine in resistant compared with susceptible Palmer amaranth (80% of applied) (Table 2; Fig. 1A). In addition, resistant plants showed greater (67%–88% of applied) ^{14}C-atrazine absorption from 4 to 72 HAT compared with susceptible plants (57%–80% of applied) (Fig. 1A). Resistant Palmer amaranth took 10.8 h to absorb 90% of the ^{14}C-atrazine, compared with 14.6 h by the susceptible plants (Table 2). Similarly, resistant plants had greater (54% of applied) maximum ^{14}C-atrazine recovered in the TL compared with susceptible plants (38%), which could be related to greater absorption in the resistant plants (Table 2; Fig. 1B). However, the resistant and susceptible biotypes took a similar time (14–15 HAT) for 90% of the maximum recovery of ^{14}C-atrazine to occur in the TL. Based on atrazine metabolism study, atrazine was metabolized at a faster rate in resistant plants, which could have resulted in greater amounts of atrazine absorption in resistant compared with susceptible plants. The absorption and translocation of resistant plants were not lower than the susceptible plants; therefore, reduced atrazine absorption or translocation does not confer non target site atrazine resistance in atrazine- and HPPD inhibitor-resistant Palmer amaranth from Nebraska. In addition, Nakka et al. (2017*a*) did not report reduced atrazine absorption and translocation as a mechanism of atrazine resistance in atrazine- and HPPD inhibitor-resistant Palmer amaranth from Kansas.

Table 2. Parameter estimates and test of lack-of-fit at 95% level for the two-parameter rectangular hyperbolic function[a] fitted to ^{14}C-atrazine absorption and ^{14}C-atrazine compounds present in treated Palmer amaranth leaves in a laboratory study conducted at Kansas State University, Manhattan, KS.

Palmer amaranth biotype	R_{max}[b]	t_{90}[b]	Lack-of-fit[c]
^{14}C-atrazine absorption (% of applied)			
Resistant	89a	10.8b	0.6
Susceptible	80b	14.6a	0.4
^{14}C-atrazine present in treated leaf (% of applied)			
Resistant	54a	15a	0.2
Susceptible	38b	14a	0.5

[a]$RH = (R_{max} \times t)/[(10/c) \times t_c + t]$, where RH describes ^{14}C-atrazine absorption (% of applied), R_{max} is the maximum percentage of the applied atrazine dose that will be absorbed at time (t), c is the arbitrary percentage (25%, 50%, or 90%) of R_{max}, and t_c represents the number of hours after treatment required to reach 25%, 50%, or 90% of the R_{max}.

[b]The predicted parameters were compared using the t test and means within columns followed by different lowercase letters are significantly different at $P \leq 0.05$.

[c]A test of lack-of-fit at the 95% level was not significant for any of the curves tested, indicating that the fitted model was correct.

^{14}C-atrazine metabolism

No effect of experimental runs or its interaction with biotype or HAT was observed for the parent ^{14}C-atrazine or its polar metabolite recovered in the TL; therefore, data were combined over two experimental runs. A significant biotype × HAT interaction was observed for ^{14}C-atrazine and the parent ^{14}C-atrazine or its metabolite

Fig. 1. (A) ^{14}C-atrazine absorption (% of applied) and (B) ^{14}C-atrazine present in the treated leaf (TL) (% of applied) of atrazine- and 4-hydroxyphenylpyruvate dioxygenase (HPPD) inhibitor-resistant and susceptible Palmer amaranth at different hours after ^{14}C-atrazine treatment in a laboratory study conducted at Kansas State University, Manhattan, KS. [Colour online.]

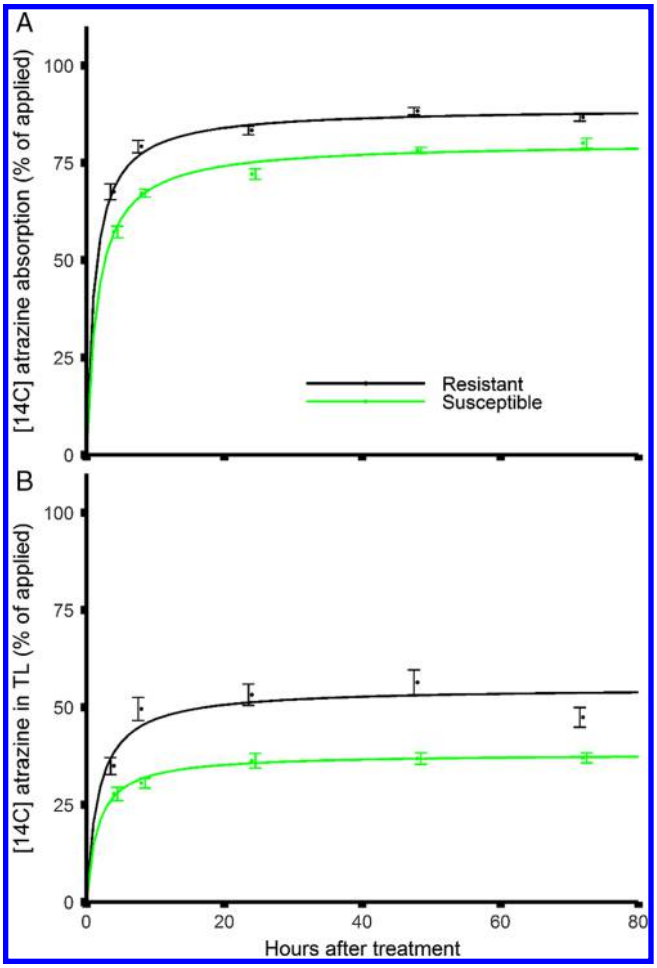

Fig. 2. (A) Parent ^{14}C-atrazine remaining in the treated leaf (% of recovered) and (B) ^{14}C-atrazine metabolite present in the treated leaf (% of recovered) of atrazine- and 4-hydroxyphenylpyruvate dioxygenase (HPPD) inhibitor-resistant and susceptible Palmer amaranth at different hours after ^{14}C-atrazine treatment in a laboratory study conducted at Kansas State University, Manhattan, KS. [Colour online.]

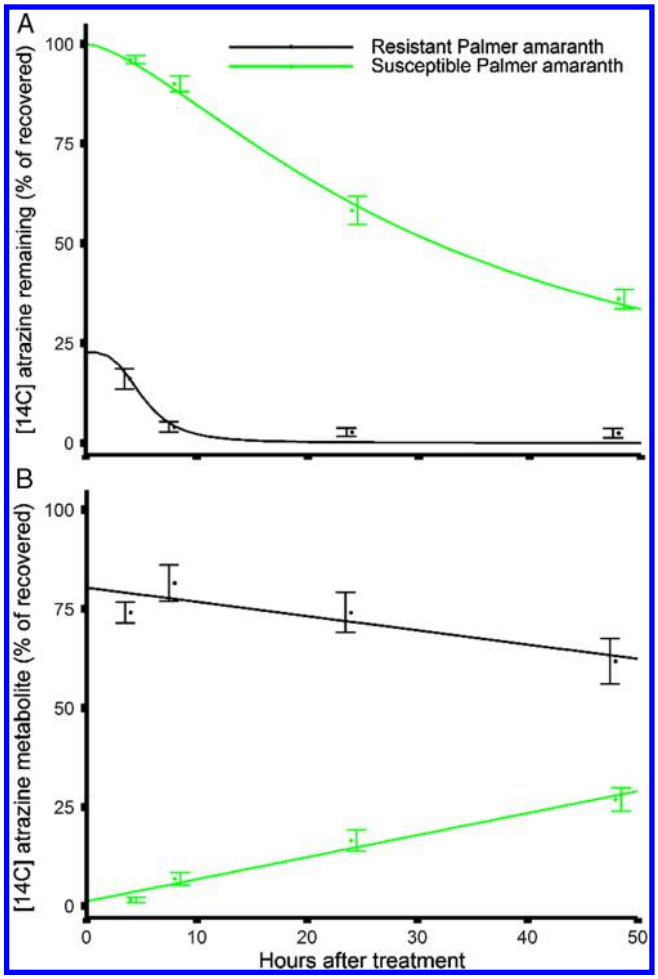

recovery in the TL; therefore, regression analysis was performed for biotypes over HAT (Fig. 2).

Metabolism-based atrazine tolerance or resistance has already been confirmed in several crops or weed species as a result of detoxification of atrazine mediated by GSTs (Shimabukuro et al. 1971; Gray et al. 1996; Cummins et al. 1999; Ma et al. 2013; Nakka et al. 2017*a*). The peak retention time of the parent ^{14}C-atrazine was observed at 19.2 min, and around 10.1 min for atrazine-GSH conjugate. The parent ^{14}C-atrazine was also observed at 19.2 min and major atrazine metabolite around 10.1 min in resistant Palmer amaranth (data not shown). Similarly, Nakka et al. (2017*a*) reported a peak retention time of parent atrazine at 18.7 min and atrazine-GSH conjugate as the major metabolite at 9.7 min in atrazine- and HPPD inhibitor-resistant Palmer amaranth from Kansas during an atrazine metabolism study. The three-parameter log-logistic model suggested that susceptible plants had greater (98% of recovered) parent ^{14}C-atrazine recovered in treated leaves at 4 HAT compared with resistant plants (22.7% of recovered), indicating atrazine metabolism or detoxification via GST as a non-target mechanism of resistance in resistant Palmer amaranth from Nebraska (Table 3; Fig. 2A). Parent ^{14}C-atrazine recovery also decreased over time in susceptible plants and only 38% of the parent ^{14}C-atrazine was recovered at 72 HAT; however, no parent ^{14}C-atrazine was recovered in resistant plants after 8 HAT (Fig. 2A). Based on the model estimation, resistant plants had a greater (75%) percentage of atrazine metabolites recovered in the treated leaves at 4 HAT compared with susceptible plants (1.2% of recovered) (Table 3; Fig. 2B), further validating atrazine metabolism or detoxification in resistant Palmer amaranth.

Table 3. Parameter estimates for the three-parameter log-logistic function[a] fitted to the parent ^{14}C-atrazine present in the treated leaf and linear model[b] fitted to the metabolites present in the treated leaf of atrazine- and 4-hydroxyphenylpyruvate dioxygenase (HPPD) inhibitor-resistant and susceptible Palmer amaranth biotypes in an atrazine metabolism study conducted at Kansas State University, Manhattan, KS.

Parent ^{14}C-atrazine present in the treated leaf (% of recovered)				
Biotype	A_{max}[c]	£[c]	b[c]	Lack-of-fit[d]
Resistant	22.7b	10a	3.3a	0.6
Susceptible	100a	7b	1.5b	0.4
^{14}C-metabolite present in the treated leaf (% of recovered)				
Biotype	β^c	α^c	R^2	
Resistant	80a	−0.36a	0.8	
Susceptible	1.2b	0.6b	0.7	

[a] $Y = \frac{A_{max}}{1+\exp[b(\log t - \log £)]}$, where Y is the parent ^{14}C-atrazine remaining in the treated leaf, A_{max} is the maximum percentage of parent ^{14}C-atrazine present in the treated leaf at time (t), £ represents the number of hours after treatment required to reach 90% of the A_{max}, and b represents the relative slope around the parameter £.

[b] $Y = \alpha x + \beta$, where Y is the percentage of the ^{14}C-atrazine metabolites recovered in the treated leaf, β is the intercept or initial ^{14}C atrazine metabolite expressed as the percentage recovered, α is the slope or rate of change of the ^{14}C-atrazine metabolite recovery over time, and x is the time expressed as hours after treatment.

[c] The predicted parameters were compared using the t test and means within columns followed by different lowercase letters are significantly different at $P \leq 0.05$.

[d] A test of lack-of-fit at the 95% level was not significant for any of the curves tested, indicating that the fitted model was correct.

Sequence of *psbA* gene

Alteration or point mutation in the *psbA* gene has contributed to atrazine resistance in several weed species such as barnyardgrass (Lopez-Martinez et al. 1997), large crabgrass (Salava et al. 2008), and wild radish (Shane Friesen and Powles 2007). To investigate point mutation in the *psbA* gene in Palmer amaranth, a 578-bp-long fragment of the *psbA* gene covering commonly known point mutations causing PS II inhibitors resistance in different weed species was amplified from susceptible and resistant Palmer amaranth from Nebraska. The sequence comparison of resistant and susceptible biotypes revealed that the $Ser_{264}Gly$ mutation that most commonly confers atrazine resistance in other weed species (Lopez-Martinez et al. 1997; Shane Friesen and Powles 2007; Salava et al. 2008; Svyantek et al. 2016) was not present (Table 4). Other amino acid substitutions such as $Phe_{255}Ile$, $Asn_{266}Thr$, or $Phe_{274}Val$ reported in the *psbA*

Table 4. Nucleotide sequence alignment of the *psbA* gene fragment from atrazine- and 4-hydroxyphenylpyruvate dioxygenase (HPPD) inhibitor-resistant (R) and susceptible (S) Palmer amaranth biotypes from Nebraska.[a]

Amino acid no.	254	**255**	256	257	258	259	260	261	262	263	**264**	265	**266**	267	268	269	270	271	272	273	**274**	275	276	277	278	279	280
Amino acid name		**PHE**									**SER**		**ASN**								**PHE**						
Consensus sequence	TAT	**TTT**	GGT	CGA	TTG	ATC	TTC	CAA	TAT	GCT	**AGT**	TTC	**AAC**	AAC	TCT	CGT	TCT	TTA	CAC	TTC	**TTC**	TTA	GCT	GCT	TGG	CCT	GTA
R-1	TAT	**TTT**	GGT	CGA	TTG	ATC	TTC	CAA	TAT	GCT	**AGT**	TTC	**AAC**	AAC	TCT	CGT	TCT	TTA	CAC	TTC	**TTC**	TTA	GCT	GCT	TGG	CCT	GTA
R-2	TAT	**TTT**	GGT	CGA	TTG	ATC	TTC	CAA	TAT	GCT	**AGT**	TTC	**AAC**	AAC	TCT	CGT	TCT	TTA	CAC	TTC	**TTC**	TTA	GCT	GCT	TGG	CCT	GTA
R-3	TAT	**TTT**	GGT	CGA	TTG	ATC	TTC	CAA	TAT	GCT	**AGT**	TTC	**AAC**	AAC	TCT	CGT	TCT	TTA	CAC	TTC	**TTC**	TTA	GCT	GCT	TGG	CCT	GTA
R-4	TAT	**TTT**	GGT	CGA	TTG	ATC	TTC	CAA	TAT	GCT	**AGT**	TTC	**AAC**	AAC	TCT	CGT	TCT	TTA	CAC	TTC	**TTC**	TTA	GCT	GCT	TGG	CCT	GTA
R-5	TAT	**TTT**	GGT	CGA	TTG	ATC	TTC	CAA	TAT	GCT	**AGT**	TTC	**AAC**	AAC	TCT	CGT	TCT	TTA	CAC	TTC	**TTC**	TTA	GCT	GCT	TGG	CCT	GTA
S-1	TAT	**TTT**	GGT	CGA	TTG	ATC	TTC	CAA	TAT	GCT	**AGT**	TTC	**AAC**	AAC	TCT	CGT	TCT	TTA	CAC	TTC	**TTC**	TTA	GCT	GCT	TGG	CCT	GTA
S-2	TAT	**TTT**	GGT	CGA	TTG	ATC	TTC	CAA	TAT	GCT	**AGT**	TTC	**AAC**	AAC	TCT	CGT	TCT	TTA	CAC	TTC	**TTC**	TTA	GCT	GCT	TGG	CCT	GTA
S-3	TAT	**TTT**	GGT	CGA	TTG	ATC	TTC	CAA	TAT	GCT	**AGT**	TTC	**AAC**	AAC	TCT	CGT	TCT	TTA	CAC	TTC	**TTC**	TTA	GCT	GCT	TGG	CCT	GTA
S-4	TAT	**TTT**	GGT	CGA	TTG	ATC	TTC	CAA	TAT	GCT	**AGT**	TTC	**AAC**	AAC	TCT	CGT	TCT	TTA	CAC	TTC	**TTC**	TTA	GCT	GCT	TGG	CCT	GTA

Note: Bold values indicate locations of PHE_{255}, SER_{264}, ASN_{266}, or PHE_{274} where mutations were previously reported in atrazine-resistant weed species.
[a] Nucleotide/amino acid numbering refers to the *Arabidopsis thaliana psbA* gene sequence.

gene conferring resistance to other PS II inhibitors such as triazinones and ureas (Park and Mallory-Smith 2006; Perez-Jones et al. 2009; Davis 2014) were also not observed in resistant Palmer amaranth (Table 4).

Conclusions

Enhanced atrazine metabolism or detoxification via GST activity was conferred as the mechanism of atrazine resistance in atrazine- and HPPD inhibitors-resistant Palmer amaranth from Nebraska. However, reduced ^{14}C-atrazine absorption and translocation or mutation in the *psbA* gene were not involved as the mechanisms of atrazine resistance. In contrast, Svyantek et al. (2016) reported reduced absorption and translocation as well as enhanced atrazine metabolism as the mechanisms of atrazine resistance in annual bluegrass. Previous studies have reported enhanced atrazine detoxification as the mechanism of resistance in different weed species (Gray et al. 1996; Cummins et al. 1999; Ma et al. 2013), including Palmer amaranth (Nakka et al. 2017*a*). Palmer amaranth from Nebraska is multiple resistant to atrazine as well as HPPD-inhibiting herbicides applied alone PRE or POST. In addition, a glyphosate-resistant Palmer amaranth biotype has also been reported in Nebraska (Chahal et al. 2017). Therefore, integrated Palmer amaranth management strategies that include the use of a PRE followed by POST herbicide program with distinct sites of action, crop rotation, tillage, or harvest weed seed control methods need to be adopted to reduce the evolution and spread of herbicide-resistant Palmer amaranth (Ganie et al. 2017*b*; Chahal and Jhala 2018; Chahal et al. 2018).

Acknowledgements

We acknowledge S. Nakka, K. Putta, A. Varanasi, J. Ou, and I. Rogers for their assistance in this project. Partial funding from the Nebraska Corn Board is highly appreciated.

References

Chahal, P.S., and Jhala, A.J. 2018. Interaction of PS II- and HPPD-inhibiting herbicides for control of Palmer amaranth (*Amaranthus palmeri*) resistant to both herbicide sites of action. Agron. J. **110**: 1–11. doi:10.2134/agronj2017.12.0704.

Chahal, P.S., Aulakh, J.S., Jugulum, M., and Jhala, A.J. 2015. Herbicide-resistant Palmer amaranth (*Amaranthus palmeri* S. Wats.) in the United States — mechanisms of resistance, impact, and management. Pages 1–29 in A. Price, ed. Herbicides, agronomic crops, and weed biology. InTech, Rijeka, Croatia.

Chahal, P.S., Varanasi, V.K., Jugulam, M., and Jhala, A.J. 2017. Glyphosate-resistant Palmer amaranth (*Amaranthus palmeri*) in Nebraska: confirmation, EPSPS gene amplification, and response to POST corn and soybean herbicides. Weed Technol. **31**: 80–93. doi:10.1614/WT-D-16-00109.1.

Chahal, P.S., Irmak, S., Gaines, T., Amundsen, K., Jugulam, M., Jha, P., et al. 2018. Control of photosystem II- and 4-hydroxyphenylpyruvate dioxygenase inhibitor-resistant Palmer amaranth (*Amaranthus palmeri*) in conventional corn. Weed Technol. **32**: 326–335. doi:10.1017/wet.2017.111.

Cummins, I., Cole, D.J., and Edwards, R. 1999. A role for glutathione transferases functioning as glutathione peroxidases in resistance to multiple herbicides in black-grass. Plant J. **18**: 285–292. doi:10.1046/j.1365-313X.1999.00452.x. PMID:10377994.

Davis, G. 2014. A survey and characterization of linuron-resistant *Amaranthus* spp. in southern Ontario carrot production. M.S. thesis, The University of Guelph, Guelph, ON.

Ganie, Z.A., Jugulam, M., and Jhala, A.J. 2017*a*. Temperature influences efficacy, absorption, and translocation of 2,4-D or glyphosate in glyphosate-resistant and glyphosate-susceptible common ragweed (*Ambrosia artemisiifolia*) and giant ragweed (*Ambrosia trifida*). Weed Sci. **65**: 588–602. doi:10.1017/wsc.2017.32.

Ganie, Z.A., Lindquist, J.L., Jugulam, M., Kruger, G., Marx, D., and Jhala, A.J. 2017*b*. An integrated approach for management of glyphosate-resistant *Ambrosia trifida* with tillage and herbicides in glyphosate-resistant corn. Weed Res. **57**: 112–122. doi:10.1111/wre.12244.

Godar, A.S., Varanasi, V.K., Nakka, S., Prasad, P.V.V., Thompson, C.R., and Mithila, J. 2015. Physiological and molecular mechanisms of differential sensitivity of Palmer amaranth (*Amaranthus palmeri*) to mesotrione at varying growth temperatures. PLoS ONE, **10**: e0126731. doi:10.1371/journal.pone.0126731. PMID:25992558.

Gray, J.A., Balke, N.E., and Stoltenberg, D.E. 1996. Increased glutathione conjugation of atrazine confers resistance in a Wisconsin velvetleaf (*Abutilon theophrasti*) biotype. Pestic. Biochem. Physiol. **55**: 157–171. doi:10.1006/pest.1996.0045.

Heap, I. 2018. Herbicide resistant Palmer amaranth globally. [Online]. Available from http://www.weedscience.org/Summary/Species.aspx [21 Sept. 2018].

Hess, F.D. 2000. Light-dependent herbicides: an overview. Weed Sci. **48**: 160–170. doi:10.1614/0043-1745(2000)048[0160:LDHAO]2.0.CO;2.

Huffman, J., Hausman, N.E., Hager, A.G., Riechers, D.E., and Tranel, P.J. 2015. Genetics and inheritance of nontarget-site resistances to atrazine and mesotrione in a waterhemp (*Amaranthus tuberculatus*) population from Illinois. Weed Sci. **63**: 799–809. doi:10.1614/WS-D-15-00055.1.

Jhala, A.J., Sandell, L.D., Rana, N., Kruger, G.R., and Knezevic, S.Z. 2014. Confirmation and control of triazine and 4-hydroxyphenylpyruvate dioxygenase-inhibiting herbicide-resistant Palmer amaranth (*Amaranthus palmeri*) in Nebraska. Weed Technol. **28**: 28–38. doi:10.1614/WT-D-13-00090.1.

Kniss, A.R., Vassios, J.D., Nissen, S.J., and Ritz, C. 2011. Nonlinear regression analysis of herbicide absorption studies. Weed Sci. **59**: 601–610. doi:10.1614/WS-D-11-00034.1.

Kohrt, J.R., and Sprague, C.L. 2017. Herbicide management strategies in field corn for a three-way herbicide-resistant Palmer amaranth (*Amaranthus palmeri*) population. Weed Technol. **31**: 364–372. doi:10.1017/wet.2017.18.

Küpper, A., Peter, F., Zöllner, P., Lorentz, L., Tranel, P.J., Beffa, R., and Gaines, T.A. 2018. Tembotrione detoxification in 4-hydroxyphenylpyruvate dioxygenase (HPPD) inhibitor-resistant Palmer amaranth (*Amaranthus palmeri* S. Wats.). Pest Manage. Sci. **74**: 2325–2334. doi:10.1002/ps.4786.

Lopez-Martinez, N., Marshall, G., and Prado, R.D. 1997. Resistance of barnyardgrass (*Echinochloa crus-galli*) to atrazine and quinclorac. Pestic. Sci. **51**: 171–175. doi:10.1002/(SICI)1096-9063(199710)51:2<171::AID-PS612>3.0.CO;2-7.

Ma, R., Kaundun, S.S., Tranel, P.J., Riggins, C.W., McGinness, D.L., Hager, A.G., et al. 2013. Distinct detoxification mechanisms confer resistance to mesotrione and atrazine in a population of waterhemp. Plant Physiol. **163**: 368–377. doi:10.1104/pp.113.223156. PMID:23872617.

Mengistu, L.W., Christoffers, M.J., and Lym, R.G. 2005. A *psbA* mutation in *Kochia scoparia* (L) Schrad from railroad

rights-of-way with resistance to diuron, tebuthiuron and metribuzin. Pest Manage. Sci. **61**: 1035–1042. doi:10.1002/ps.1079.

Nakka, S., Godar, A.S., Thompson, C.R., Peterson, D.E., and Jugulam, M. 2017*a*. Rapid detoxification via glutathione S-transferase (GST) conjugation confers a high level of atrazine resistance in Palmer amaranth (*Amaranthus palmeri*). Pest Manage. Sci. **73**: 2236–2243. doi:10.1002/ps.4615.

Nakka, S., Godar, A.S., Wani, P.S., Thompson, C.R., Peterson, D.E., Roelofs, J., and Jugulam, M. 2017*b*. Physiological and molecular characterization of hydroxyphenylpyruvate dioxygenase (HPPD)-inhibitor resistance in Palmer amaranth (*Amaranthus palmeri* S. Wats.). Front. Plant Sci. **8**: 555. doi:10.3389/fpls.2017.00555. PMID:28443128.

Park, K.W., and Mallory-Smith, C.A. 2006. *psbA* mutation (Asn_{266} to Thr) in *Senecio vulgaris* L. confers resistance to several PSII-inhibiting herbicides. Pest Manage. Sci. **62**: 880–885. doi:10.1002/ps.1252.

Perez-Jones, A., Intanon, S., and Mallory-Smith, C. 2009. Molecular analysis of hexazinone-resistant shepherd's-purse (*Capsella bursa-pastoris*) reveals a novel *psbA* mutation. Weed Sci. **57**: 574–578. doi:10.1614/WS-09-089.1.

Ritz, C., and Streibig, J.C. 2016. Analysis of dose-response curves. [Online]. Available from https://cran.r-project.org/web/packages/drc/drc.pdf.

Salava, J., Kocová, M., Holá, D., Rothová, O., Nováková, K., and Chodová, D. 2008. Identification of the mechanism of atrazine resistance in a Czech large crabgrass biotype. J. Plant Dis. Prot. **21**: 101–104.

Shane Friesen, L.J., and Powles, S.B. 2007. Physiological and molecular characterization of atrazine resistance in a wild radish (*Raphanus raphanistrum*) population. Weed Technol. **21**: 910–914. doi:10.1614/WT-07-008.1.

Shimabukuro, R., Frear, D., Swanson, H., and Walsh, W. 1971. Glutathione conjugation an enzymatic basis for atrazine resistance in corn. Plant Physiol. **47**: 10–14. doi:10.1104/pp.47.1.10. PMID:5543779.

Svyantek, A.W., Aldahir, P., Chen, S., Flessner, M.L., McCullough, P.E., Sidhu, S.S., and McElroy, J.S. 2016. Target and nontarget resistance mechanisms induce annual bluegrass (*Poa annua*) resistance to atrazine, amicarbazone, and diuron. Weed Technol. **30**: 773–782. doi:10.1614/WT-D-15-00173.1.

This article has been cited by:

1. Jugulam, Shyam. 2019. Non-Target-Site Resistance to Herbicides: Recent Developments. *Plants* **8**:10, 417. [Crossref]